J. Membrane Biol. 170, 191–203 (1999)

The Journal of
Membrane
Biology

The Role of MIP in Lens Fiber Cell Membrane Transport

K. Varadaraj[1], C. Kushmerick[3], G.J. Baldo[1], S. Bassnett[2], A. Shiels[2], R.T. Mathias[1]

[1]Department of Physiology and Biophysics, SUNY at Stony Brook, Stony Brook, NY 11794-8661, USA
[2]Department of Ophthalmology and Visual Sciences, Washington University School of Medicine, St. Louis, MO 63110, USA
[3]Departmento de Farmacologia, Institute Ciencias Biologicas, Universidade Federal de Minas Gerais, Pampulha, Belo Horizonte 31270-901, Brasil

Received: 17 February 1999/Revised: 16 April 1999

Abstract. MIP has been hypothesized to be a gap junction protein, a membrane ion channel, a membrane water channel and a facilitator of glycerol transport and metabolism. These possible roles have been indirectly suggested by the localization of MIP in lens gap junctional plaques and the properties of MIP when reconstituted into artificial membranes or exogenously expressed in oocytes. We have examined lens fiber cells to see if these functions are present and whether they are affected by a mutation of MIP found in Cat^{Fr} mouse lens. Of these five hypothesized functions, only one, the role of water channel, appears to be true of fiber cells *in situ.* Based on the rate of volume change of vesicles placed in a hypertonic solution, fiber cell membrane lipids have a low water permeability (p_{H2O}) on the order of 1 μm/sec whereas normal fiber cell membrane p_{H2O} was 17 μm/sec frog, 32 μm/sec rabbit and 43 μm/sec mouse. Cat^{Fr} mouse lens fiber cell p_{H2O} was reduced by 13 μm/sec for heterozygous and 30 μm/sec for homozygous mutants when compared to wild type. Lastly, when expressed in oocytes, the p_{H2O} conferred by MIP is not sensitive to Hg^{2+} whereas that of CHIP28 (AQP1) is blocked by Hg^{2+}. The fiber cell membrane p_{H2O} was also not sensitive to Hg^{2+} whereas lens epithelial cell p_{H2O} (136 μm/sec in rabbit) was blocked by Hg^{2+}. With regard to the other hypothesized roles, fiber cell membrane or lipid vesicles had a glycerol permeability on the order of 1 nm/sec, an order of magnitude less than that conferred by MIP when expressed in oocytes. Impedance studies were employed to determine gap junctional coupling and fiber cell membrane conductance in wild-type and heterozygous Cat^{Fr} mouse lenses. There was no detectable difference in either coupling or conductance between the wild-type and the mutant lenses.

Key words: Lens — MIP — Aquaporins — Water permeability — Glycerol permeability — Cat^{Fr} mouse

Introduction

The ocular lens comprises a single layer of epithelial cells on its anterior surface and fiber cells that make up its volume (Benedetti et al., 1976). Equatorial epithelial cells continuously elongate and differentiate into a layer of new fiber cells, which cover the older fiber cells. Thus the oldest fibers are at the center of the lens. During the process of differentiation, many new cytoplasmic and membrane proteins are synthesized while many of the old epithelial proteins are degraded. The most abundant new membrane protein is MIP (or MP26 or AQP0), which is synthesized as a 28 kDa protein in differentiating equatorial cells. Once the fiber cells mature, MIP is subjected to proteolysis and the N- and C-termini are cleaved, producing a 22 kD form. MIP is thought to be unique to lens fiber cells, where it is over 60% of total membrane protein (Broekhuyse, Kuhlmann & Stols, 1976).

Many roles have been proposed for MIP. Initially, because of its localization in gap junctional plaques (Bok, Dockstader & Horwitz, 1982; FitzGerald, Bok & Horwitz, 1983), MIP was thought to contribute to cell-to-cell coupling. However, when cloned and sequenced (Gorin et al., 1984), there was little homology found between MIP and gap junction proteins (connexins). Moreover, expression of MIP in *Xenopus* oocytes (Swenson et al., 1989; Kushmerick et al., 1995) did not produce coupling.

Correspondence to: R.T. Mathias

Abbreviations: MIP, Major Intrinsic Protein of Lens; AQP, Aquaporins

When reconstituted into bilayers (Ehring et al., 1990) or liposomes (Gooden et al., 1985; Nikaido & Rosenberg, 1985; Girsch & Peracchia, 1985; Peracchia & Girsch, 1989; Shen et al., 1991), MIP formed a relatively nonselective, large conductance ion channel, thus leading to the hypothesis that this was its role in the lens. However, fiber cell membranes have an exceptionally high resistance to ion flow (reviewed in Mathias, Rae & Baldo, 1997), so if MIP were an ion channel, it must have a very low open probability. Furthermore, when MIP was expressed in *Xenopus* oocytes, Kushmerick et al. (1995) found no effect on the membrane resistance to ion flow.

MIP is a member of the aquaporin (AQP) family of membrane transport proteins (reviewed in Chepelinsky (1994) or Park & Saier, 1996). Other members of this family have been shown to act as transmembrane water channels or glycerol transporters. When expressed in *Xenopus* oocytes, MIP increased membrane water permeability (Kushmerick et al., 1995; Mulders et al., 1995; Zampighi et al., 1995; Yang & Verkman, 1997; Chandy et al., 1997). The most commonly found aquaporin is AQP1 (or CHIP28, Agre et al., 1993), which is expressed in lens epithelial cells (Bondy et al., 1993; Agre et al., 1993). The water permeability of AQP1 is much greater than that of MIP and it is blocked by Hg^{2+} (Chandy et al., 1997), whereas the water permeability of MIP is not blocked by Hg^{2+} (Kushmerick et al., 1995; Mulders et al., 1995).

Some members of the AQP family specifically transport small neutral solutes (discussed in Park & Saier (1996). Kushmerick et al. (1995) examined the effect of expression of MIP on oocyte transport of various neutral solutes (glycerol, sucrose, glucose, inositol, sorbitol, glutathione and urea). Of these, only glycerol transport was increased by the presence of MIP. Another member of the AQP family, GlpF (Maurel et al., 1994), specifically facilitates glycerol transport. Thus, Kushmerick, Varadaraj & Mathias (1998) further investigated the effect of MIP on glycerol transport and metabolism in oocytes and found MIP increased both glycerol permeability and the activity of the glycerol kinase.

The above data suggest four potential roles for MIP in fiber cell membrane transport: (i) a cell-to-cell channel in gap junctions; (ii) a nonselective ion channel; (iii) a water channel; (iv) a glycerol transporter. In addition, since MIP enhances the activity of the glycerol kinase, it might have a role in fiber cell membrane synthesis. The purpose of this study was to find evidence either for or against each of these roles in the lens. To do so, we examined the transport properties of vesicles formed from normal fiber cell membrane, and from fiber cell membrane of the Cat^{Fr} mutant mouse lens. These mice synthesize a mutated form of MIP that has an abnormal C-terminus and is poorly translocated to the fiber cell membrane (Shiels & Bassnett, 1996; Shiels, Collis & Bassnett, 1999).

Materials and Methods

Male rabbits (New Zealand White; 1.3 kg) were sacrificed by intravenous injection of sodium pentobarbitone solution into a marginal ear vein. Mice were sacrificed by intraperitoneal injection of pentobarbitone (720 mg/kg body weight). Frogs were sacrificed by pithing. These procedures are approved by the American Association for Accreditation of Laboratory Animal Care (AAALAC). Eyeballs were excised and placed in calcium free physiological lens saline solution: for mammalian lenses (in mM): NaCl 150, KCl 4.7, $MgCl_2$ 1, glucose 5, HEPES 5, pH 7.4); and for frog lenses, (NaCl 108.5, KCl 2.5, $MgCl_2$ 1.5, HEPES 5, pH 7.4). Intact lenses were dissected immediately and capsules and epithelial layers were removed. In the larger rabbit lenses, outer and inner cortical layers and nuclei were separated by dissection.

Preparation of Rabbit Lens Epithelial Cells

Lens capsules were pooled and incubated in collagenase dissociation buffer (in mM): Na-aspartate 150, KCl 4.7, glucose 5, HEPES 5, pH 7.4, 0.125% collagenase (Type IV, Worthington Biochemical, Freehold, NJ)) for 30 min at 32°C. Each capsule was gently removed from the enzyme solution and placed in 1 ml of normal mammalian lens saline without Ca^{2+}. Epithelial cells were gently removed from the capsules by gentle trituration with a transfer pipette and the cells were pelleted (150 × *g* for 5–8 min) and resuspended in 200 μl of calcium-free mammalian physiological saline. Osmolarity of the saline solution was determined using a micro-osmometer (Advanced Instruments, MA).

Preparation of Lens Fiber Cell Vesicles

Lens fiber cells were manually teased out from anterior to posterior sutures using a tweezers. The isolated clumps of fiber cells were incubated for 1 hr in the lens physiological saline solution containing 0.5 mM $CaCl_2$, then triturated gently using a rocking platform. The integrity of vesicles was determined as described in Pasquale et al. (1990). Vesicles were incubated in the membrane permeant dye BCECF-AM, which was cleaved by intracellular esterases trapped in the vesicles. The vesicles containing the membrane impermeant, fluorescent BCECF retained significant fluorescence on the following day, suggesting their membranes were intact.

Immunofluorescent Localization of MIP

Rabbit lens fiber cells and vesicles were immunostained to confirm the presence of intact MIP in the membrane. Fiber cells and vesicles were spread on poly-L-lysine coated glass slide (Electron Microscopy Sciences, PA) and allowed to settle for 30 min. Samples were fixed in ice-cold freshly prepared 2% paraformaldehyde/0.1% Triton X-100 in PBS (in mM): NaCl 137; KCl 2.7; $Na_2HPO_4.7H_2O$ 10; KH_2PO_4 1.4; pH 7.2 for 30 min. Slides were washed twice in PBS at 4°C for 5 min each then incubated overnight with a mouse monoclonal antibody (2 μg/ml) against bovine MIP (gift from Dr. P. FitzGerald, University of California, Davis, CA; FitzGerald et al., 1983). Slides were washed twice in PBS and exposed to fluorescein isothiocyanate (FITC) labeled, goat anti-mouse IgG, (Vector Labs, CA) for 1 hr at room temperature in the

dark. They were washed twice in PBS and photographed using an epifluorescence microscope with an excitation band pass filter of 465–495 nm and an emission band pass filter of 515–555 nm.

Preparation of Lens Lipids

Lipids were extracted using a modified method of Folch (1957) one-phase alcohol solvent system, using methanol-chloroform-water (Bligh & Dyer, 1959) as described by Kates (1986). All solutions were bubbled with argon and extraction was carried out in an atmosphere of argon where possible. Lens tissues were homogenized initially in distilled H_2O (0.5 ml/g wet weight). The homogenates were then extracted with organic solvents. Lipid was concentrated and dried completely in a rotary evaporator at 35°C in the presence of benzene to remove any trace of water present. The lipid was redissolved in hexane-isopropanol (1:1, v/v) and centrifuged to eliminate nonprotein impurities (Sato et al., 1996). Lipid was concentrated and dried completely as mentioned above. The lipid residue was dissolved in chloroform-methanol (2:1, v/v) and stored under argon at −80°C. The lipid fraction was separated into classes by thin-layer chromatography (TLC; silica-G) using a hexane:ether:glacial acetic acid (80:20:1) solvent system (Kates, 1986). Lipids were visualized with I_2 vapor. Lipid classes were identified based on their mobility in comparison with lipid standards (Sigma, St. Louis, MO).

Preparation of Giant Unilamellar Lens Lipid Vesicles

Vesicles from lens lipids were prepared using a modified method of Akashi et al. (1996). The lipid samples were dissolved in chloroform and methanol (2:1, v/v). The evaporator-flask (10 ml) was cleaned well with soap, washed with distilled H_2O, dried and washed again in hexane, dried under argon and baked at 250°C for 2 hr to ensure uniform spreading of lipid on the glass surface. To form a thin film of lipid, the chloroform and methanol-lipid mix was dried at 40°C in a rotary evaporator. To remove the last traces of organic solvents in the lipid film, the flask was kept under vacuum for 12 hr in darkness. The lipid film was prehydrated with water-saturated nitrogen at 40°C for 35 min. To hydrate the lipid film, 4 ml of the buffer solution (10 mM KCl and 100 mM sucrose which had been argon-purged) was added gently; the flask was sealed under argon and incubated at 40°C for about 20 hr. During incubation, the flask was rocked gently for 30 min at 4-hr intervals to strip the dried lipid film from the inner surface of the flask. Lipid vesicles were harvested and stored under argon in the dark at 6°C and used as soon as possible. However, lipid vesicles were stable for more than a week. To attach the vesicles to poly-L-lysine coated cover glass, the vesicle preparation was diluted with 60 mM KCl at a ratio of 1:2 and spun down at 500 rpm for 20 min at 4°C in an Eppendorf centrifuge. The supernatant was discarded and the vesicles were suspended in 60 mM KCl.

Lens Impedance Studies

Impedance studies were carried out as described in Mathias, Rae & Eisenberg (1981). Briefly, the lens was dissected from the eye with four flaps of scleral tissue attached. The flaps were pinned into a sylgard lined bath and the lens was impaled with two intracellular microelectrodes. A centrally placed microelectrode injected a wide-band stochastic current. The induced voltage was recorded using a peripherally placed microelectrode. The circuits and shielding procedures were exactly as described in Mathias et al. (1981). The current and voltage signals were recorded with a Fast Fourier Analyzer (Hewlett Packard Model 3562A) and the impedance computed in real time. The impedance data and a calibration curve, which was recorded for each microelectrode, were sent to an IBM PC where the data were calibrated for artifactual phase shift, then curve fit with an equivalent circuit model to obtain the fiber cell membrane conductance and gap junctional coupling conductance.

List of Symbols

$a(t)$	cm	Radius of a sphere that approximates the shape of the vesicle cell.
$A(t)$	cm^2	Observed cross sectional area of the vesicle or cell.
$c_i(t)$	M	Internal concentration of impermeant solutes (e.g., ions or larger molecules).
c_o	M	External concentration of impermeant solutes.
c_{H2O}	M	Concentration of water ≈55 M
D	cm^2/sec	Diffusion constant for the external solute.
$Gly_i(t)$	M	Internal concentration of glycerol.
Gly_o	M	External concentration of glycerol.
p_{Gly}	cm/sec	Membrane permeability of glycerol.
p_{H2O}	cm/sec	Membrane permeability of water.
S_m	cm^2	Surface area of membrane for the vesicle or cell.
t	sec	Time.
$V_i(t)$	cm^3	Internal volume of the vesicle or cell.
V_1	cm^3	Initial volume of the vesicle or cell determined by curve fitting.
V_2	cm^3	Final volume of the vesicle or cell determined by curve fitting.
Δc_o	M	Local change in external concentration at the surface of the vesicle or cell.
τ	sec	Time constant of the change in volume determined by curve fitting.

Estimation of Surface Area and Volume

We determined membrane water and glycerol permeabilities using digital video microscopy to estimate volume changes and the membrane surface area of the vesicle or cell. An image of the cross section of a vesicle/cell was digitized using a Videoscope image intensifier and an Ikegami digital video camera. The image was transferred to a PC using a Data Translation DT-2851 video frame grabber. Epithelial cell images were stored to disk at the maximum rate of 1 every 2 sec, whereas fiber cell membrane and lipid vesicle images were stored at slower rates that depended on their rate of volume change. The cross sectional area at any time ($A(t)$ cm^2) was determined by tracing and counting pixels using Sigma Scan/Image Analysis. At any time t, an effective radius, $a(t)$ cm, of a sphere was computed from:

$$a(t) = \sqrt{\frac{A(t)}{\pi}} \tag{1}$$

The membrane surface area (S_m cm^2) was estimated from the initial observation of $A(0)$, before the vesicle/cell underwent any osmotically induced shrinkage:

$$S_m = 4\pi a^2(0) \tag{2}$$

The volume of the vesicle/cell ($V_i(t)$ cm^3) was estimated from:

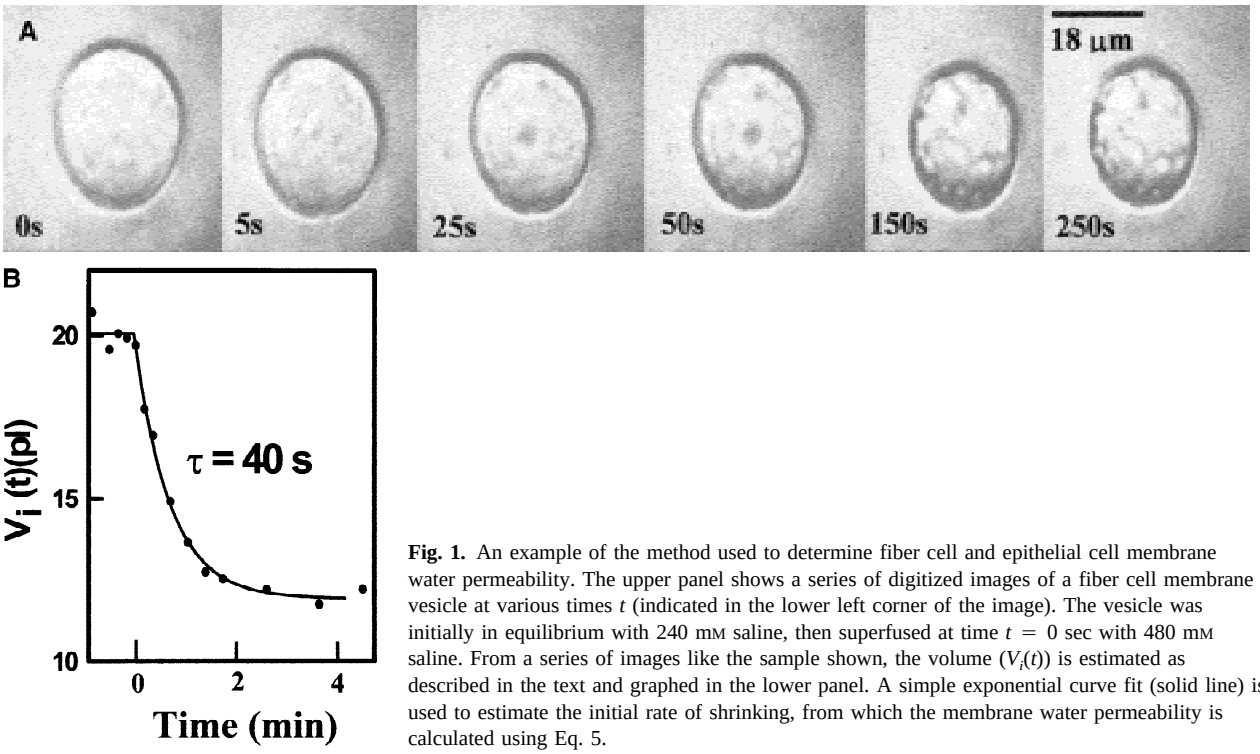

Fig. 1. An example of the method used to determine fiber cell and epithelial cell membrane water permeability. The upper panel shows a series of digitized images of a fiber cell membrane vesicle at various times t (indicated in the lower left corner of the image). The vesicle was initially in equilibrium with 240 mM saline, then superfused at time $t = 0$ sec with 480 mM saline. From a series of images like the sample shown, the volume ($V_i(t)$) is estimated as described in the text and graphed in the lower panel. A simple exponential curve fit (solid line) is used to estimate the initial rate of shrinking, from which the membrane water permeability is calculated using Eq. 5.

$$V_i(t) = \frac{4}{3}\pi a^3(t) \tag{3}$$

The obvious limitation of this technique is that is uses a 2-dimensional image to predict a 3-dimensional structure. Since the shape in the third dimension is not known, the cross section is used to predict the surface and volume of a sphere. When we used a stereo microscope and viewed the vesicles/cells from a limited set of angles, they appeared to be spheroidal. As can be seen in Fig. 1, a typical cross section is approximately an ellipse with a ratio of minor to major axes of about 0.8. If this image is rotated in the third dimension to form a prolate spheroid, our spherical approximation will over estimate S_m by a factor of 1.05 and over estimate V_i by 1.12. However, our estimate of p_{H2O} will only be in error by a factor of 1.06 because it depends on the ratio V_i/S_m. Conversely, if the image is rotated to form an oblate spheroid, our spherical approximation will under estimate S_m by 0.92, under estimate V_i by 0.89 and under estimate p_{H2O} by 0.97.

Water Permeability

Figure 1 shows a series of photos of a membrane vesicle shrinking with time following a change in bath osmolarity from 240 mM to 480 mM saline. The time constant for changing our bath was approximately 0.8 sec. This particular vesicle was from a frog lens. Although most of our studies were on mammalian lens fiber cell vesicles, the appearance of a vesicle was the same regardless of species. Below the photos is a graph of the estimated volume *vs.* time. We assume water flows in proportion to the difference in external osmolarity (c_o M) and internal osmolarity ($c_i(t)$ M), at a rate determined by the membrane water permeability (p_{H2O} cm/sec). Thus the volume ($V_i(t)$ cm^3) follows the equation:

$$c_{H2O}\frac{dV_i(t)}{dt} = S_m\, p_{H2O}(c_i(t) - c_o) \tag{4}$$

where $c_{H2O} \approx 55$ M is the concentration of water. The water permeability can be estimated from the initial rate of volume change.

$$p_{H2O} = \frac{1}{S_m}\frac{c_{H2O}}{c_i(0) - c_o}\frac{dV_i(0)}{dt} \tag{5}$$

For the example in Fig. 1, $c_i(0) = 240$ mM, since the vesicle was initially in equilibrium with a bath containing 240 mM saline and $c_o = 480$ mM.

To determine the initial rate of volume change, $V_i(t)$ data were curve fit with the arbitrary equation:

$$V_i(t) = V_2 - (V_2 - V_1)e^{-t/\tau} \tag{6}$$

Using the best fit values V_1, V_2 and τ, the initial rate of change is given by:

$$\frac{dV_i(0)}{dt} = \frac{V_2 - V_1}{\tau} \tag{7}$$

Using the best parameters, Eq. 7 was substituted into Eq. 5 to obtain p_{H2O}. For the vesicle in Fig. 1, p_{H2O} was 13 μm/sec.

There is at least one potential problem with this method. When water flows through a membrane, it convects solute up to one side and away from the other, thus reducing the actual transmembrane osmotic gradient. The maximum concentration change would occur when convection and diffusion balance during maximum water flow. As described in Kushmerick et al. (1995), this worst case change in external concentration (Δc_o M) is described by:

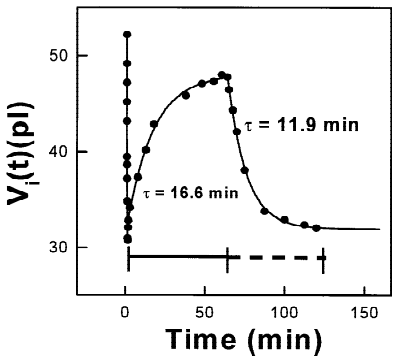

Fig. 2. The complete time course of volume changes for a fiber cell membrane vesicle in a typical experiment to determine glycerol permeability. The vesicle was initially in equilibrium with a bathing solution containing 300 mM saline. At time $t = 0$ sec the bath is changed to one containing 300 mM saline plus 300 mM glycerol (solid line beneath the curve). Because the osmolarity was doubled, the vesicle rapidly loses water and shrinks to about ½ its initial volume, then glycerol begins to diffuse across the membrane and water follows, causing a relatively slow recovery toward its initial volume. The glycerol permeability is calculated from the initial rate of swelling using Eq. 14. After about an hour, the vesicle has equilibrated with the bath and a second solution change is made. The external glycerol is replaced with impermeant mannitol (dashed line beneath the curve), causing the volume to slowly reshrink as the glycerol diffuses out of the vesicle. The glycerol permeability was estimated a second time from the initial rate of reshrinking using Eq. 16.

$$\Delta c_o = c_o \exp\left\{\frac{a(0)p_{H2O}}{Dc_{H2O}}(c_i(0) - c_o)\right\} \tag{8}$$

where the diffusion coefficient $D \approx 10^{-5}$ cm^2/sec. Using the largest values of $a(0)$ and p_{H2O} for either vesicles or cells, we conclude $\Delta c_o \leq$ 1.5 mM and is typically less than 1 mM. These changes will have negligible effect on our determination of p_{H2O}.

Glycerol Permeability

Figure 2 shows a typical time course of vesicle volume changes during a glycerol permeability study. This vesicle was from a rabbit lens. The vesicle was initially in equilibrium with a bath containing 300 mM saline. The bath was switched to one containing 300 mM saline plus 300 mM glycerol (c_o = 300 mM, Gly_o = 300 mM, total osmolarity = 600 mM). The increase in bath osmolarity causes in initial efflux of water and the vesicle rapidly shrinks. We assume the entry of glycerol is negligible in this initial rapid phase of shrinking. If so, the vesicle should shrink to 50% of its initial volume. In this experiment the estimated change was to 56% of initial volume, indicating our assumption is reasonable. Thus at the time when the vesicle begins to recover, the initial conditions are:

$$\begin{aligned} c_i(0) &= 600 \text{ mM} \\ & \text{swelling} \\ Gly_i(0) &= 0 \text{ mM} \end{aligned} \tag{9}$$

Because water is much more permeant than glycerol, once the initial phase of shrinking is complete, we assume water stays in equilibrium. Thus,

$$c_i(t) + Gly_i(t) = c_o + Gly_o \tag{10}$$

Glycerol now diffuses into the vesicle, down its concentration gradient, at a rate determined by p_{Gly}

$$\frac{d(V_i(t)Gly_i(t))}{dt} = S_m p_{Gly}(Gly_o - Gly_i(t)) \tag{11}$$

We assume ions can be treated as impermeant solutes on the time scale of glycerol diffusion, thus the number of moles of ions within the vesicle is constant:

$$\frac{d(V_i(t)c_i(t))}{dt} = 0 \tag{12}$$

Solving Eq. 10 for $Gly_i(t)$ and substituting into the left hand side of Eq. 11, given Eq. 12, we obtain

$$(c_o + Gly_o)\frac{dV_i(t)}{dt} = S_m p_{Gly}(Gly_o - Gly_i(t)) \quad \text{swelling} \tag{13}$$

For the swelling in Figure 2, p_{Gly} is estimated using Eq. 13 with the initial conditions in Eq. 9

$$p_{Gly} = \frac{c_o + Gly_o}{S_m Gly_o}\frac{dV_i(0)}{dt} \qquad \text{swelling} \tag{14}$$

where $t = 0$ is defined as the time the swelling begins. The value of $dV_i(0)/dt$ was determined as described for water permeability (*see* the text around Eqs. 6 and 7).

When the vesicle reaches a new steady-state volume, both glycerol and water are in equilibrium and, in theory, the volume should return to its initial value. In this experiment the estimated volume returned to 90% of its initial value. In the final phase of this experiment, we removed glycerol from the bath but kept the osmolarity constant at 600 mM using manitol as an impermeant substitute for glycerol. Thus $Gly_o = 0$ mM and $c_o = 600$ mM. In these conditions, glycerol diffuses out of the vesicle and water follows, causing the vesicle to reshrink at a rate determined by p_{Gly}. We redefine $t = 0$ as the time the reshrinking begins and assign the initial conditions:

$$\begin{aligned} Gly_i(0) &= 300 \text{ mM} \\ & \text{reshrinking} \\ c_i(0) &= 300 \text{ mM} \end{aligned} \tag{15}$$

Again substituting Eq. 10 in Eq. 11 but with the initial conditions in Eq. 15, we obtain

$$p_{Gly} = -\frac{c_o}{S_m Gly_i(0)}\frac{dV_i(0)}{dt} \qquad \text{reshrinking} \tag{16}$$

In either Eq. 14 or Eq. 16, the ratio of concentrations is 2, hence $dV_i(0)/dt$ should be the same but in opposite directions. Analysis of the data in Fig. 2 gives

$$\begin{aligned} p_{Gly} &= 5 \text{ nm/sec} \quad \text{swelling} \\ p_{Gly} &= 7 \text{ nm/sec} \quad \text{reshrinking} \end{aligned} \tag{17}$$

These particular values are in reasonable agreement. In Results, the average values of p_{Gly} determined from swelling or reshrinking are not significantly different.

The fiber cell membrane or lipid vesicles consistently behaved as shown in Fig. 2. The epithelial cells, however, did not consistently behave in this manner. These cells have a much higher membrane conductance than fiber cells and they appeared to implement a volume

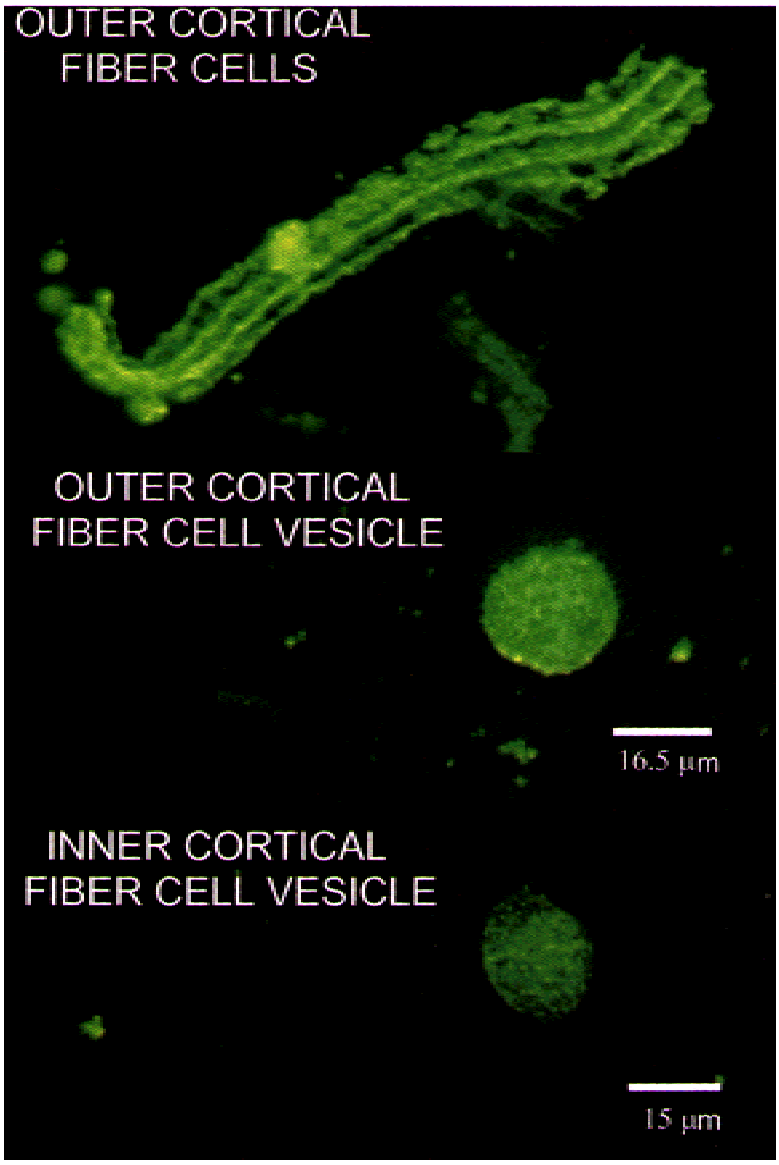

Fig. 3. Fiber cells and fiber cell membrane vesicles stained positively for MIP. These rabbit lens cells or vesicles were incubated with a mouse monoclonal antibody against an epitope on the C-terminus of bovine MIP (a gift from Dr. P. FitzGerald). They were then exposed to FITC-labeled anti-mouse IgG and the resulting fluorescence is shown.

regulatory response within the time course of the glycerol entry or exit. The initial shrinkage, as water exited, was similar but faster than that seen in Fig. 2, however the slow swelling response was not a simple, monotonic exponential. For this reason, we were not confident that the above theory would apply, so no results on p_{Gly} for epithelial cells are presented.

Results

Lens Fiber Cell Membrane Vesicles

Because MIP may change as the fibers age and become internalized, we attempted to segregate membrane vesicles from outer cortical, inner cortical and nuclear fiber cells of the relatively large rabbit lenses. However, we were unsuccessful with regard to nuclear fibers. These regional classifications were not precise, but in a rabbit lens with a radius of approximately 3 mm, the outer ~0.7 mm shell of fibers was considered outer cortex, a shell from about 0.7 to 1.7 mm into the lens was considered inner cortex, and the nucleus had a radius of about 1.3 mm. The amount of vesicles produced from inner cortical fiber cell membrane was about 50% of that from outer cortical, and we were unable to obtain any vesicles from the nuclear region.

Figure 3 shows an isolated clump of fiber cells (upper panel), a vesicle from outer cortical membrane (middle panel) and a vesicle from inner cortical membrane (lower panel), all immunostained with a mouse monoclonal antibody against the C-terminus of bovine MIP. Both inner and outer cortical membrane vesicles

stained positively for MIP, however the intensity of staining for inner vesicles was consistently less than that for outer vesicles. This difference may relate to the proteolytic cleavage of the C-terminus of MIP as the fibers age, but it might also be due to elongation of fibers with age reducing the density of MIP in the inner cortical membrane.

Vesicles such as those shown in Fig. 3 remained intact for hours, as long as the external Ca^{2+}-concentration was kept near zero, whereas in normal extracellular Ca^{2+}, they quickly disintegrated. Thus, all of the permeability studies reported below were in low external Ca^{2+}. When healthy appearing vesicles were incubated with the membrane permeant dye BCECF-AM, the dye was internalized and cleaved by intracellular esterases trapped in the vesicles to its fluorescent form, BCECF. These vesicles retained fluorescence over night, indicating their membranes were intact.

Water Permeability

Water permeability (p_{H2O}) was determined from experimental estimates of the membrane surface area and the initial rate of shrinking of vesicles or epithelial cells when the bath osmolarity was abruptly increased. For frog lens membrane vesicles, the osmolarity was changed from 240 to 480 mM, for mammalian lens membrane vesicles or epithelial cells, the osmolarity was changed from 300 to 450 mM, and for the less permeable lipid vesicles the change was from 120 to 300 mM. The method of analysis is described in Theory, where a typical volume change for a frog lens fiber cell membrane vesicle is shown. Our pilot studies for this project utilized frog lenses. Once the techniques were established, we shifted to mammalian lenses, however we first obtained good measurements from 4 vesicles made from frog lens fiber cell membrane. Their average p_{H2O} was 17 ± 5 μm/sec.

Figure 4 summarizes results from normal rabbit lens fiber cell membrane or lipid vesicles. Each panel shows a set of typical experimental determinations of volume *vs.* time and the best fit curve using Eq. 6. Above each graph is the mean ± SD for p_{H2O}. Figure 4*A* shows data from vesicles made of outer cortical fiber cell membrane. For the particular experiment shown, p_{H2O} was 33 μm/sec and the average p_{H2O} from 12 vesicles was 32 ± 7 μm/sec. Figure 4*B* shows results for inner cortical membrane vesicles. For the particular experiment shown, p_{H2O} was 8 μm/sec and the average from 7 vesicles was 10 ± 4 μm/sec.

The p_{H2O} of inner fiber cell membrane is significantly lower than that of the outer fiber cells. Recall that immunostaining for MIP was less intense in the inner fiber cell vesicles than outer. Moreover, based on the single channel water permeability of MIP and the density

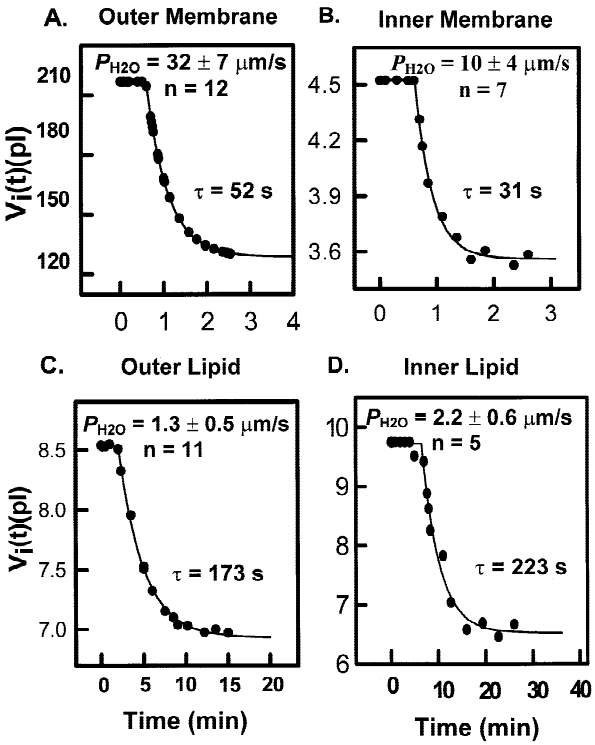

Fig. 4. The water permeability (p_{H2O}) of fiber cell membrane and lipids from rabbit lenses. The rabbit lenses were sufficiently large that fibers from the outer cortex (panels *A* and *C*) could be separated from those from the inner cortex (panels *B* and *D*). Panels *A* and *B* illustrate typical results and average ± SD values of p_{H2O} of fiber cell membrane. Panels *C* and *D* illustrate typical results and average SD values of p_{H2O} of fiber cell lipids.

of MIP in fiber cell membrane (*see* Discussion) the order of magnitude of p_{H2O} reported here corresponds to the expected contribution of MIP. Thus there is correlative evidence that the values of p_{H2O} for fiber cell membrane could be due to MIP. However, the values reported here are similar to those of pure lipid bilayers made from phosphatidylcholine (Finkelstein, 1987, Table 6–1, p. 99). Hence the question arises: Is the permeability due to MIP, or some other protein, or is it simply due to the lipid matrix? There is no known specific blocker for the water permeability of MIP, so as an alternative, we extracted all protein from the fiber cell membrane, then formed large unilamellar vesicles from the pure lipid. Figure 4*C* shows results for vesicles made of outer cortical fiber cell membrane lipids. For the particular experiment shown, the value of p_{H2O} was 1.6 μm/sec and the average value from 11 vesicles was 1.3 ± 0.5 μm/sec. Figure 4*D* shows results for inner cortical lipids. For the particular experiment shown, the value of p_{H2O} was 2 μm/sec and the average value from 5 vesicles was 2.2 ± 0.6 μm/sec. These relatively low values of lipid water permeability may be due to the relatively high concentrations of cholesterol and sphingomyelin in fiber cell

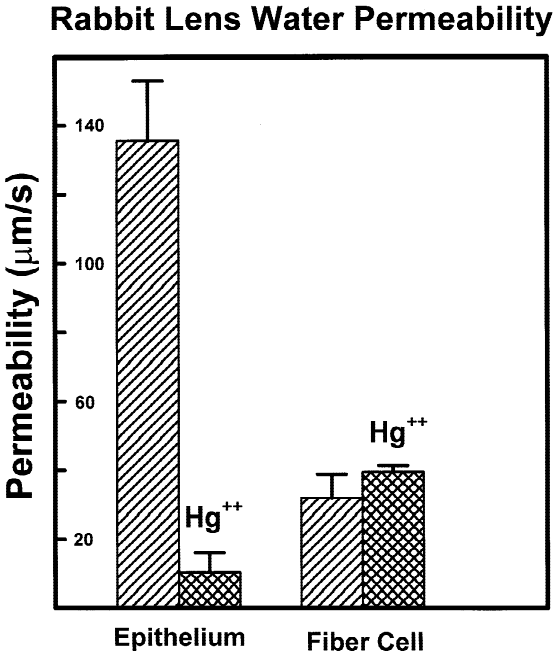

Fig. 5. A comparison of epithelial and fiber cell membrane water permeabilities. Lens epithelial cells have a relatively large water permeability that is blocked by Hg^+ whereas fiber cells have a smaller, Hg^+-insensitive water permeability. These data are consistent with CHIP28 (AQP1) being the epithelial membrane water channel and MIP being the fiber cell membrane water channel.

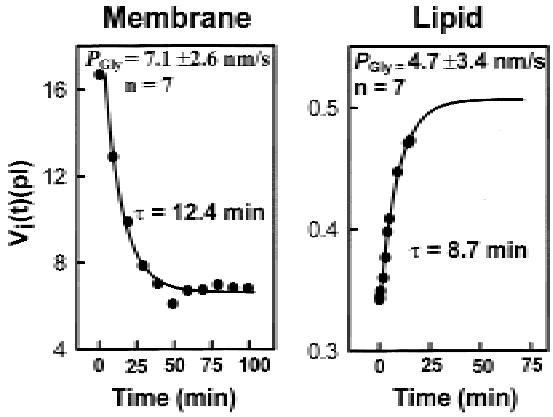

Fig. 6. The glycerol permeability (p_{Gly}) of fiber cell membrane and lipids from the outer cortex of the rabbit lens. Each panel shows a typical result and gives the mean ± SD from *n* vesicles. As described in Theory, each vesicle was first observed to swell in an isosmotic solution containing glycerol, then, if the vesicle survived, observed to reshrink in an isosmotic solution with the glycerol removed. There was no systemic difference in the values of p_{Gly} determined from swelling or reshrinking, hence a typical response of each is illustrated. The majority of fiber cell membrane glycerol permeability appears to be mediated by the lipid matrix.

membrane (Zelenka, 1984). Finkelstein (1987, Table 6–1, p. 99) lists water permeabilities for lipid bilayers of various compositions, and the one made of sphingomyelin and cholesterol had a permeability of 0.8 μm/sec. Thus our results appear to be consistent with these other studies. We conclude that the background water permeability of the lipid matrix of fiber cell membrane is about an order of magnitude less than the membrane water permeability, hence the majority of the water flow is protein mediated. Since MIP is the most abundant membrane protein, and since it is a known water channel, it is the most likely protein to mediate this permeability. If this hypothesis is correct, then the fiber cell membrane water permeability should not be blocked by Hg^{2+}, which blocks the water permeability of AQP1 (Agre et al., 1993) but not that of MIP (Kushmerick et al., 1995).

Figure 5 shows the effect of Hg^{2+} on fiber cell membrane and epithelial cell membrane water permeabilities. AQP1 is present in the epithelial cell membrane (Bondy et al., 1993; Agre et al., 1993). The single channel water permeability of AQP1 is about an order of magnitude greater than that of MIP and it is blocked by Hg^{2+} whereas that of MIP is not. The rabbit lens epithelial cell membrane p_{H2O} was 136 ± 17 μm/sec ($n = 7$) and reduced to 10 ± 6 μm/sec by 1 mM Hg^{2+}, whereas the fiber cell membrane p_{H2O} was 33 ± 7 μm/sec and not affected by Hg^{2+}. Thus, all of the data in this section are consistent with MIP being the fiber cell membrane water channel and AQP1 being the epithelial cell membrane water channel. Moreover, the presence of protein mediated water channels appears critical, since the background water permeability of lens lipids is small. There may, of course, be fiber cell membrane proteins other than MIP that also mediate water permeability, however the data in Fig. 5 rule out any of the Hg^{2+}-sensitive aquaporins.

Glycerol Permeability

Glycerol permeability (p_{Gly}) was determined as described in the Theory section. Since water is about 3 orders of magnitude more permeant than glycerol, as glycerol diffuses into or out of a vesicle in an isosmotic solution, water follows at essentially the same rate. The rate of volume change is therefore proportional to p_{Gly}. The left hand panel of Fig. 6 shows the volume reduction of an outer cortical fiber cell membrane vesicle, initially loaded with 300 mM glycerol plus 300 mM saline, after it was placed in isosmotic (300 mM saline plus 300 mM mannitol) solution containing no glycerol. For the experiment shown, p_{Gly} was 8.5 nm/sec and in 7 vesicles the average p_{Gly} was 7.1 ± 2.6 nm/sec. As in the water permeability study, we extracted all the membrane protein and selected unilamellar vesicles for our studies of outer cortical fiber cell membrane lipids. The right hand panel of Fig. 6 shows a graph of the volume of such a lipid vesicle that initially contained 240 mM impermeant

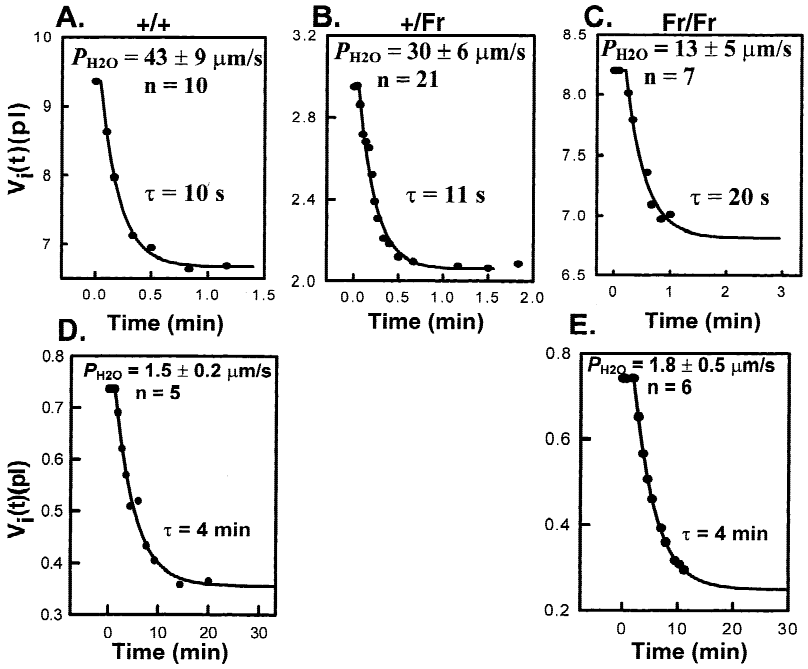

Fig. 7. The water permeability (p_{H2O}) of fiber cell membrane and lipids from wild-type (+/+) mouse lenses and heterozygous (+/Fr) and homozygous (Fr/Fr) Cat^{Fr} mutant mouse lenses. Each panel shows a typical result and gives the mean ± SD from *n* vesicles. The Cat^{Fr} mouse synthesizes a mutant form of MIP that is poorly translocated to the fiber cell membrane. This mutation has no significant effect on the p_{H2O} of fiber cell lipids (panel *D* and *E*), however, the systematic reduction in the amount of MIP present in +/+, +/Fr, and Fr/Fr mouse lenses results in a systematic decrease in p_{H2O}.

solute (no glycerol), then swelled when placed in a solution containing 120 mM impermeant solute plus 120 mM glycerol. For the vesicle shown, the value of p_{Gly} was 5.1 nm/sec and the average of 7 vesicles was 4.7 ± 3.4 nm/sec. In contrast to the result on water permeability, the background lipid permeability for glycerol appears to be responsible for the majority of the fiber cell membrane p_{Gly}.

In oocytes, frog lens MIP induced a p_{Gly} of about 15 nm/sec, which is at least an order of magnitude greater than the p_{Gly} reported here for rabbit lens MIP. Although the sequence of MIP is fairly well conserved, it was possible that this was a species related difference. We therefore looked at membrane vesicles from fiber cells of the frog lens and determined p_{Gly} was 2.9 ± 1.3 nm/sec (n = 10). Thus, the lack of glycerol permeability is probably a general property of MIP in its normal environment of fiber cell membrane.

Results From the CAT^{FR} Mouse Lens Fiber Cells

The Cat^{Fr} mouse synthesizes a mutated form of MIP that is poorly translocated to the fiber cell membrane (Shields et al., 1999). The lenses from homozygous (Fr/Fr) mice are undersized and are mostly opaque. These proved impossible to use for microelectrode based, whole lens impedance studies, however the heterozygous mutants (+/Fr) express less normal MIP than control (+/+) and have lenses that appear more normal and could be used for such studies. For the water permeability studies described below, we were able to form vesicles from membranes or lipids located in the cortex of normal appearing fibers from Fr/Fr mouse lenses, as well as from +/+ and +/Fr lenses. These +/+, +/Fr and Fr/Fr mice allowed us to study the effects of reductions in MIP on fiber cell membrane conductance, fiber cell gap junctional coupling and fiber cell membrane water permeability.

Water Permeability

Figure 7 summarizes our results on the water permeability of fiber cell membrane (Panels *A, B* and *C*) and fiber cell lipids (Panels *D* and *E*). Each panel illustrates a typical result and the average ± SD for *n* vesicles. The data in panel *A* are from membrane vesicles made from cortical lens fibers of control mice. For the experiment shown, the value of p_{H2O} was 43 μm/sec and the average from 10 vesicles was 43 ± 9 μm/sec. Panel *B* shows results from heterozygous mutant Cat^{Fr} mouse lenses, which have less normal MIP than controls. For the experiment shown, p_{H2O} was 28 μm/sec and the average from 21 vesicles was 30 ± 6 μm/sec. Panel *C* represents homozygous mutants that lack normal MIP. The particular experiment shown gave a value of p_{H2O} of 12 μm/sec and the average of 7 vesicles was 13 ± 5 μm/sec. Thus, the lack of normal MIP in Fr/Fr mouse lenses reduced the average p_{H2O} by 30 μm/sec, about twice the reduction in +/Fr lenses. Panel *D* shows the background lipid water permeability of +/+ mice. For the particular vesicle represented in *D*, the p_{H2O} was 1.5 μm/sec and the average from 5 vesicles was 1.5 ± 0.2 μm/sec. The p_{H2O} in the absence of normal MIP (panel *C*) is signifi-

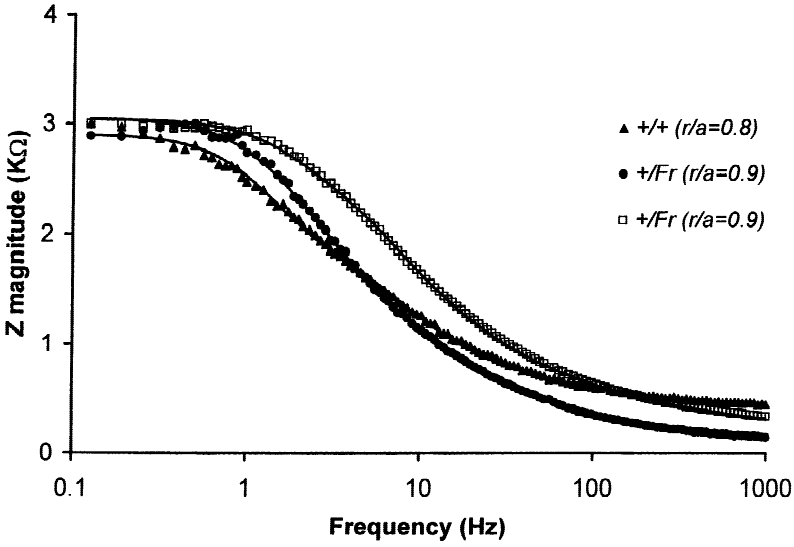

Fig. 8. The magnitude of the impedance or input resistance of a wild-type (+/+) mouse lens and two heterozygous (+/Fr) Cat^{Fr} mutant mouse lenses. Based on curve fits (solid lines) of these data, the reduced amount of MIP in the +/Fr lenses has no detectable effect on gap junctional coupling or fiber cell conductance.

cantly larger than that of the normal lipids. This might be due to: (1) mutant MIP that was translocated into the plasma membrane, (2) other membrane proteins, or (3) an altered the lipid composition resulting in a higher background permeability. However, as can be seen in panel *E*, the fiber cell lipid water permeability from Fr/Fr mice is the same as +/+. The particular experiment shown in *E* gave a p_{H2O} of 2.0 μm/sec and the average from 6 vesicles was 1.8 ± 0.5 μm/sec. Thus, insofar as water permeability is concerned, a lack of normal MIP does not appear to affect the fiber cell lipids. With regard to the first two possibilities, the Cat^{Fr} mutation to MIP is in the C-terminus, hence our antibody does not recognize the mutant form and we could not determine how much, if any, MIP was in the fiber cell membrane of Fr/Fr mice. Therefore, we do not know whether the water permeability in panel C is due to mutated MIP or some other protein.

Fiber Cell Gap Junctional and Membrane Conductances

Figure 8 shows the input resistance of intact lenses as a function of the sinusoidal frequency of the injected current. The current was injected into a centrally located fiber cell. The voltage electrode was inserted at a distance half way between the posterior pole and equator and moved inward into a fiber at a distance *r* (cm) from the center of a lens with radius *a* (cm). The input resistance depends on both the radius and the location of the voltage recording microelectrode, however, the lenses all had similar radii of around 1 mm, and the voltage was recorded at similar *r*-locations that were 100–300 μm from the surface. The smooth curves were generated by curve fitting the impedance data with a structurally based model of the electrical properties of the lens (Mathias et al., 1981). The curve fitting allowed us to estimate the gap junctional conductance between fibers in the shell located between the point of recording the voltage and the surface of the lens, and also provided an estimate of the average membrane conductance of the fiber cells.

The data in Fig. 8 are from two different +/Fr lenses and one normal +/+ lens. The input resistance as frequency approaches zero is virtually identical for the three lenses and the frequency dependence of the three curves is not significantly different, even though the +/Fr lenses showed a very significant reduction in water permeability, consistent with a reduction in the amount of normal MIP in the fiber cell membrane. To accurately determine the gap junctional coupling conductance, we would have had to map the impedance at multiple locations between the anterior and posterior poles, and at multiple depths into the lens (Baldo & Mathias, 1992). This would have been a formidable task, since these small lenses did not survive multiple penetrations with the voltage electrode. However, to compare gap junctional coupling in +/+ and +/Fr mouse lenses, we curve fit the data at one location with a model for the average (from pole to pole) conductance coupling fibers in an outer shell about 300 μm thick. The values of the effective intracellular resistivity for this shell were 2.6 ± 1.5 KΩ-cm ($n = 12$) for +/+ mice, and 2.3 ± 0.6 KΩ-cm ($n = 8$) for +/Fr mice. These values are obviously not different and indicate an average cell to cell coupling conductance of 1–2 S/cm^2, assuming the fiber cells are 3 μm thick. To unambiguously determine fiber cell membrane conductance, we need morphometric data on the amount of fiber cell membrane per unit volume of tissue, and such data were not available for mouse lenses. To deal with the lack of morphometric data, we report the average fiber cell membrane conductance per μF of membrane capacitance. We assume these fiber cells, like

those of frog or rat lenses (Mathias et al., 1997), have a membrane capacitance of about 1 $\mu F/cm^2$. Our curve fitting detected no significant difference in the fiber cell membrane capacitance of +/+ and +/Fr mouse lenses and the best fit values of fiber cell membrane conductance were 4.8 ± 4.0 $\mu S/\mu F$ for +/+ mice and 4.8 ± 3.4 $\mu S/\mu F$ for +/Fr mice. There is no indication from these data that a reduction in the amount of MIP in the fiber cell membrane has any effect on gap junctional conductance or membrane conductance.

Discussion

Of the various roles hypothesized for MIP, only water transport appears to carry over to lens fiber cells. The p_{H2O} of fiber cell membrane is almost entirely mediated by protein, since it is more than an order of magnitude greater than that of the background lipid matrix, and the most abundant membrane protein is MIP. Moreover, the p_{H2O} of fiber membrane was insensitive to Hg^{2+} as was the p_{H2O} of MIP in oocytes (Kushmerick et al., 1995) and reductions in p_{H2O} correlated with reductions of MIP in the Cat^{Fr} mouse lenses. Lastly, based on the single channel water permeability of MIP and the density of MIP in fiber cell membrane, Chandy et al. (1997) predicted a fiber cell membrane p_{H2O} due to MIP on the order of 10 μm/sec. Our measured values of p_{H2O} are this order of magnitude, suggesting MIP is the water channel. Although all this evidence is indirect and correlative, in total it makes a strong case for MIP being the fiber cell membrane water channel.

The small glycerol permeability of lens fiber cell membrane was surprising. In oocytes, expression of frog lens MIP caused an increase in glycerol permeability (p_{Gly}) of about 15 nm/sec (Kushmerick et al., 1995, 1998) and an increase in oocyte water permeability of 12 μm/sec. Thus while the fiber cell membrane p_{H2O} is generally larger than that induced by MIP in oocytes, the fiber cell p_{Gly} of 7.1 nm/sec in rabbit is significantly smaller. Moreover, the majority of the rabbit lens fiber cell p_{Gly} appears to arise from the lipid matrix, which had a p_{Gly} of 4.7 nm/sec. When we looked at frog lens p_{Gly} it was only 2.9 nm/sec, suggesting the lack of glycerol permeability is not species related. Indeed, given the standard deviations in the rabbit lens fiber cell p_{Gly} (about ± 3 nm/sec), it is not obvious that MIP contributes any glycerol permeability in the lens. Perhaps the glycerol permeability induced in oocytes is a residual property of the aquaporins. In the lens, this function may be eliminated by some post translational event.

Another observation in oocytes (Kushmerick et al., 1998) was that MIP increased the activity of the glycerol kinase. This led to the speculation that MIP could have a role in fiber cell membrane synthesis or anaerobic metabolism of glycerol. Although our data on the water permeability of fiber cell lipids do not rule out a role in membrane synthesis, they do not support it. The water permeability of fiber cell lipids is unusually low when compared to most biomembranes, probably due to relatively high concentrations of sphingomyelin and cholesterol (Zelenka, 1984; Finkelstein, 1987, Table 6–1, p. 99). When we compared the water permeability of lipids from fiber cells of normal mouse lenses with the permeability of lipids from Fr/Fr mouse lenses, there was no significant difference, suggesting no difference in lipid composition.

As was reviewed in Introduction, early studies suggested MIP might be a gap junction channel or a membrane ion channel. However enthusiasm for these hypotheses has waned since these functions were not found when MIP was expressed in oocytes (Kushmerick et al., 1995). Moreover, the sequence of MIP (Gorin et al., 1984) indicates it is a member of the aquaporin family rather than the connexin family (Chepelinsky, 1994). Although the prevailing opinion at this time is that MIP is not a gap junction channel, its presence in fiber cell gap junctional plaques (FitzGerald et al., 1983) means it could have some other role in fiber cell gap junctions. However we found no effect on fiber gap junctional coupling when we compared wild-type and heterozygous (+/Fr) mutant mouse lenses. Shiels et al. (1999) suggest that +/Fr lenses have less normal MIP than +/+ lenses, and that the mutant MIP is largely trapped in the endoplasmic reticulum. We found a reduced water permeability of fiber cell membrane from +/Fr lenses as compared to +/+ lenses, consistent with the +/Fr lenses having less MIP than normal. Thus, if MIP had a role in gap junctional coupling, we should have seen some difference between the +/+ and +/Fr mice.

The best fit values of fiber cell membrane conductance were identical in +/+ and +/Fr lenses, each being 4.8 $\mu sec/\mu F$ but with a standard deviation of about ±4 $\mu sec/\mu F$. Perhaps a more convincing argument against MIP influencing membrane resistance is that the input resistances of +/+ and +/Fr lenses is the same. The curve fitting process attempts to parse the resistance between surface cell membrane, fiber cell membrane and the high resistance, small extracellular spaces between fibers. The process of parsing out the contributions is not exact, but if MIP had any significant role in fiber cell membrane resistance, one would expect the +/Fr mouse lens to have a significantly higher input resistance than the +/+ mouse lens.

The data presented here suggest MIP has a physiological role as the fiber cell membrane water channel, whereas AQP1 appears to play a similar role in lens epithelial cells. We have not measured water flow in an intact lens, however Fischbarg et al. (1999) have shown tissue cultured sheets of lens epithelial cells transport fluid, and Mathias et al. (1997) suggested fluid might

follow the standing ion fluxes that circulate through the lens. There are considerable data on the standing ion fluxes (reviewed by Mathias et al., 1997). The data suggest the large current entering the lens at both poles and exiting at the equator is primarily a Na^+ flux. The current is thought to enter the lens along the extracellular spaces between fiber cells. It eventually crosses into a fiber cell through Na^+-leak channels, then leaves that fiber cell by gap junctions, which direct the flux from cell to cell to the equatorial surface, where the Na^+ is transported out of the lens by Na/K pumps. Both K^+- and Cl^--currents are also present, and the component of current carried by Cl^- will reduce the net solute flux. However, if we ignore any component of the circulating current carried by Cl^-, the maximum net solute flux entering a fiber cell is $j_m = i_m/F$, where i_m is the value of current entering the cell. The question we wish to address is whether the values of p_{H2O} measured here are sufficiently large to generate fluid flow that is essentially isotonic with the maximum possible solute fluxes.

Isotonic water flow is the maximum limit that is approached as the membrane water permeability approaches infinity, transmembrane osmotic gradients approach zero and the solute flux (j_m) divided by the water flow (u_m) approaches the osmolarity of the bath (c_o):$c_o = j_m/u_m$. Assuming $j_m = i_m/F$, for a typical lens fiber cell, $j_m = 3$ pmoles/(cm^2 sec) and $c_o = 300$ mM, thus the limit on water flow can be estimated from $u_m = j_m/c_o$, which is 0.1 nm/sec. If there is indeed a fiber cell transmembrane water flow that approaches this limiting value, then the transmembrane osmotic gradient (Δc_m) needed to drive such a flow must be small. In general, $u_m = p_{H2O}\,\Delta c_m/C_{H2O}$, where $c_{H2O} \approx 55$ M is the concentration of water and we have measured $p_{H2O} \approx 20$ μm/sec for fiber cell membrane. The osmotic gradient needed to generate a 0.1 nm/sec water flow is therefore less than 0.3 mM, which is insignificant in comparison to the 300 mM concentration of solute around the cells. Thus the standing Na^+ current should generate fluid flow that is essentially isotonic. At the lens surface, the Na^+ efflux is concentrated in equatorial epithelial cells where the current density is on the order of 20 μA/cm^2 giving a net solute efflux of 200 pmols/(cm^2 sec), which is much larger than the average influx per fiber cell. However, the p_{H2O} of epithelial cells is 136 μm/sec, which is much greater than that of fiber cells. For water to isotonically follow the epithelial cell solute efflux, a transmembrane osmotic gradient of about 2.7 mM would need to exist. Again, relative to a 300 mM osmolarity of the external solution, this is quite small and suggests that the standing, circulating flux of Na^+ will generate a similar pattern of water flow that is essentially isotonic.

Based on the above calculations, the presence of MIP in fiber cells seems marginally critical to lens water flow. However, our estimate of fiber cell membrane solute flux could easily be in error, and if the flux were 10 times greater in some local domain of fibers, the p_{H2O} of MIP would be more critical. Nevertheless, the complete degeneration of lenses in Fr/Fr mice seems too dramatic to be simply related to a reduced p_{H2O} of fiber cell membrane. Perhaps MIP has roles other than acting as a water channel. This study has been primarily directed at the role of MIP in fiber cell membrane transport. The only role of MIP in membrane transport appears to be that of a water channel, but it could obviously have other important roles, for example in lens structure, development, or some function not yet considered.

This work was supported by National Institutes of Health grants EY06391 and EY11411.

References

Agre, P., Preston, G.M., Smith, B.L., Jung, J.S., Raina, S., Moon, C., Guggion, W.B., Nielsen, S. 1993. Aquaporin CHIP: the archetypal molecular water channel. *Am. J. Physiol.* **265:**F463–F476

Akashi, K-I., Mijata, H., Itoh, H., Kinosita, K., Jr. 1996. Preparation of giant liposomes in physiological conditions and their characterization under an optical microscope. *Biophys. J.* **71:**3242–3250

Baldo, G.J., Mathias, R.T. 1992. Spatial variations in membrane properties in the intact rat lens. *Biophys. J.* **63:**518–529

Benedetti, E.L., Dunia, I., Bentzel, C.J., Vermorken, A.J.M., Kibbelaar, M., Bloemendal, H. 1976. A portrait of plasma membrane specializations in eye lens epithelium and fibers. *Biochem. Biophys. Acta* **457:**353–384

Bligh, E.G., Dyer, W.J. 1959. A rapid method of total lipid extraction and purification. *Can. J. Biochem. Physiol.* **31:**911–917

Bok, D., Dockstader, J., Horwitz, J. 1982. Immunocytochemical localization of the lens main intrinsic polupeptide (MIP26) in ultrathin frozen sections of rat lens. *J. Cell Biol.* **92:**213–220

Bondy, C., Chin, E., Smith, B.L., Preston, G.M., Agre, P. 1993. Developmental gene expression and tissue distribution of CHIP28 water-channel protein. *Proc. Natl. Acad. Sci. USA* **90:**4500–4504

Broekhuyse, R.M., Kuhlmann, E.D., Stols, A.L. 1976. Lens membrane II. isolation and characterization of the main intrinsic polypeptide (MIP) of bovine lens fiber membranes. *Exp. Eye Res.* **23:**365–371

Chandy, G., Zampighi, G.A., Kreman, M., Hall, J.E. 1997. Comparison of the water transporting properties of MIP and AQP1. *J. Membrane Biol.* **159:**29–39

Chepelinsky, A.B. 1994. The MIP transmembrane channel gene family. *In:* Handbook of Membrane Channels. pp. 413–432. Academic Press, New York

Ehring, G.R., Zampighi, G., Horwitz, J., Bok, D., Hall, J.E. 1990. Properties of channel reconstituted from the major intrinsic protein of lens fiber membranes. *J. Gen. Physiol.* **96:**631–664

Finkelstein, A. 1987. Water movement through lipid bilayers, pores, and plasma membranes theory and reality. *In:* Distinguished Lecture Series of the Society of General Physiologists, Vol. 4, pp. 91–201. John Wiley & Sons, New York

Fischbarg, J., Diecke, F.P.J., Kuang, K., Yu, B., Kang, F., Iserovich, P., Li, Y., Rosskothen, H., Koniarrek, J.P. 1999. Transport of fluid by lens epithelium. *Am. J. Physiol.* **276:**C548–C557

Fitzgerald, P.G., Bok, D., Horwitz, J. 1983. Immunocytochemical localization of the main intrinsic polypeptide (MIP26) in ultra thin frozen sections of rat lens. *J. Cell Biol.* **97:**1491–1499

Folch, J., Lees, M., Sloane-Stanley, G.A. 1957. A simple method for

the isolation and purification of total lipids from animal tissues. *J. Biol. Chem.* **226:**497–509

Girsch, S.J., Peracchia, C. 1985. Lens cell-to-cell channel protein: I. self-assembly into liposomes and permeability regulation by calmodulin. *J. Membrane Biol.* **83:**217–225

Gooden, M., Rintoul, D., Takehanan, M., Takemoto, L. 1985. Major intrinsic polypeptide (MIP26K) from lens membrane: reconstitution into vesicle and inhibition of channel forming activity by peptide antiserum. *Biochem. Biophys. Res. Commun.* **128:**993–999

Gorin, M.B., Yancey, S.B., Cline, J., Revel, J.P., Horwitz, J. 1984. The major intrinsic protein (MIP) of the bovine lens fiber membrane: characterization and structure based on cDNA cloning. *Cell* **39:**49–59

Kates, M. 1986. Techniques of Lipidology. Laboratory Techniques in Biochemistry and Molecular Biology. R.H. Burdon and P.H. van Knippenberg, editors. Vol. 3, pp. 100–111. Elsevier, New York

Kushmerick, C., Rice, S.J., Baldo, G.J., Haspel, H.C., Mathias, R.T. 1995. Ion, water, neutral solute transport in *Xenopus* oocytes expressing frog lens MIP. *Exp. Eye Res.* **61:**351–362

Kushmerick, C., Varadaraj, K., Mathias, R.T. 1998. Effects of lens major intrinsic protein on glycerol permeability and metabolism. *J. Membrane Biol.* **161:**9–19

Mathias, R.T., Rae, J.L., Baldo, G.J. 1997. Physiological properties of the normal lens. *Physiol. Rev.* **77:**21–50

Mathias, R.T., Rae, J.L., Eisenberg, R.S. 1981. The lens as a nonuniform spherical synctium. *Biophys. J.* **34:**61–83

Maurel, C., Reizer, J., Schroeder, J.I., Chrispeels, M.J., Saier, M.H. 1994. Functional characterization of the *Escherichia coli* glycerol facilitator, GlpF, in *Xenopus* oocytes. *J. Biol. Chem.* **289:**11869–11872

Mulders, S.M., Preston, G.M., Deen, P.M.T., Guggino, W.G., An Os, C.D., Agre, P. 1995. Water channel properties of major intrinsic protein of lens. *J. Biol. Chem.* **270:**9010–9016

Nikaido, H., Rosenberg, E.Y. 1985. Functional reconstitution of lens gap junction proteins into proteoliposomes. *J. Membrane Biol.* **85:**87–92

Park, J.H., Saier, M.H. Jr. 1996. Phylogenetic characterization of the MIP family of transmembrane channel proteins. *J. Membrane Biol.* **153:**171–180

Pasquale, L.R., Mathias, R.T., Austin, L.R., Brink, P.R., Ciunga, M. 1990. Electrostatic properties of fiber cell membrane from the from lens. *Biophys. J.* **58:**939–945

Peracchia, C., Girsch, S.J. 1989. Calmodulin site at the C-terminus of the putative lens gap junction protein MIP26. *Lens & Eye Toxicity Res.* **6:**613–621

Sato, H., Borchman, D., Ozaki, Y., Lamba, O.P., Byrdwell, W.C., Yappert, M.C., Paterson, C.A. 1996. Lipid-protein interactions in human and bovine lens membranes by Fourier transform Raman and infrared spectroscopies. *Exp. Eye Res.* **62:**47–53

Shen, L., Shrager, P., Girsch, S.J., Donaldson, P.J., Peracchia, C. 1991. Channel reconstitution in liposomes and planar bilayers with HPLC-purified MIP26 of bovine lens. *J. Membrane Biol.* **124:**21–32

Shiels, A., Bassnett, S. 1996. Mutations in the founder of the MIP gene family underlie cataract development in the mouse. *Nature Genetics* **12:**212–215

Shiels, A., Collis, H., Bassnett, S. 1999. Transposin mutagenesis and intracellular misrouting of lens Major Intrinsic Protein (MIP) in the cataract Fraser (Cat^{Fr}) mouse. *Invest. Ophthal. & Vis. Sci.* **40:**s878

Swenson, K.I., Jordan, J.R., Beyer, E.C., Paul, D.L. 1989. Formation of gap junctions by expression of connexin in *Xenopus* oocyte pairs. *Cell* **57:**145–155

Yang, B., Verkman, A.S. 1997. Water and glycerol permeabilities of aquaporins 1–5 and MIP determined quantitatively by expression of epitope-tagged constructs in *Xenopus* oocytes. *J. Biol. Chem.* **272:**16140–16146

Zampighi, G.A., Kreman, M., Boorer, K.J., Loo, D.D.F., Bezanilla, F., Chandy, G., Hall, J.E., Wright, E.M. 1995. A method for determining the unitary functional capacity of cloned channels and transporters expressed in *Xenopus laevis* oocytes. *J. Membrane Biol.* **148:**65–78

Zelenka, P.S. 1984. Lens lipids. *Curr. Eye Res.* **3:**1337–1359